OPEN

Citation: Cell Death and Disease (2014) 5, e1291; doi:10.1038/cddis.2014.251
© 2014 Macmillan Publishers Limited   All rights reserved 2041-4889/14
www.nature.com/cddis

npg

Bcl-xL controls a switch between cell death modes during mitotic arrest

N Bah[1], L Maillet[1], J Ryan[2], S Dubreil[1], F Gautier[1,3,4], A Letai[2], P Juin[1,3] and S Barillé-Nion*,[1]

Antimitotic agents such as microtubule inhibitors (paclitaxel) are widely used in cancer therapy while new agents blocking mitosis onset are currently in development. All these agents impose a prolonged mitotic arrest in cancer cells that relies on sustained activation of the spindle assembly checkpoint and may lead to subsequent cell death by incompletely understood molecular events. We have investigated the role played by anti-apoptotic Bcl-2 family members in the fate of mitotically arrested mammary tumor cells treated with paclitaxel, or depleted in Cdc20, the activator of the anaphase promoting complex. Under these conditions, a weak and delayed mitotic cell death occurs that is caspase- and Bax/Bak-independent. Moreover, BH3 profiling assays indicate that viable cells during mitotic arrest are primed to die by apoptosis and that Bcl-xL is required to maintain mitochondrial integrity. Consistently, Bcl-xL depletion, or treatment with its inhibitor ABT-737 (but not with the specific Bcl-2 inhibitor ABT-199), during mitotic arrest converts cell response to antimitotics to efficient caspase and Bax-dependent apoptosis. Apoptotic priming under conditions of mitotic arrest relies, at least in part, on the phosphorylation on serine 62 of Bcl-xL, which modulates its interaction with Bax and its sensitivity to ABT-737. The phospho-mimetic S62D-Bcl-xL mutant is indeed less efficient than the corresponding phospho-deficient S62A-Bcl-xL mutant in sequestrating Bax and in protecting cancer cells from mitotic cell death or yeast cells from Bax-induced growth inhibition. Our results provide a rationale for combining Bcl-xL targeting to antimitotic agents to improve clinical efficacy of antimitotic strategy in cancer therapy.
Cell Death and Disease (2014) **5,** e1291; doi:10.1038/cddis.2014.251; published online 12 June 2014

Systemic chemotherapy remains the basis of cancer treatment and agents that disrupt mitotic spindle assembly are commonly used to treat a wide variety of cancers. These agents include the microtubule poisons taxanes that have proven successful in particular in breast cancer treatment. However, patient response remains highly unpredictable and drug resistance is common. By blocking microtubule dynamics, taxanes trigger chronic activation of the mitotic checkpoint leading to the inactivation of the E3-ubiquitine ligase complex anaphase-promoting complex/cyclosome relying on the sequestration of its activator Cdc20. A high level of cyclin B1 and a subsequent chronic cyclin-dependent kinase 1 activity are then responsible for the sustained mitotic arrest.[1] Previous studies reported various cellular outcomes in reponse to antimitotics including death in mitosis or mitotic exit without cell division and return to interphase (process called mitotic slippage), followed by cell cycle arrest, death or re-replication.[2,3] However, the factors that control cell fates during mitotic arrest remain incompletely understood. Gascoigne and Taylor suggested that mitotic cell death or slippage can be viewed as two competing pathways one involving the activation of cell death process and the other the degradation of cyclin B1.[4] Consistent with this model, *in vitro*

experiments increasing mitotic slippage protect cells from mitotic cell death, in addition those enhancing survival upon mitotic arrest facilitates mitotic slippage.[5] Of importance, failure to initiate apoptosis during mitotic arrest appears to be a major factor limiting the efficacy of antimitotic drugs not only in experiments using cancer cell lines but also in human breast cancers where it correlates with poor tumor response.[6] Thus, we focused our work on defining how cell death commitment occurs during a prolonged mitotic arrest, and on identifying specific molecular vulnerability of cancer cells in this situation. To decipher the molecular events that determine cell fate in response to prolonged mitotic arrest, we investigated whether mitotic arrested cells were prone to trigger apoptosis signalling and how this signalling was controlled.

Mitochondrial outer membrane permeabilization (MOMP) is the committed step of apoptotic cell death, and correlates with cancer cells' response to chemotherapy. It is highly regulated by the Bcl-2 family of proteins that contain at least one of four homology domains called BH domains and regulate life/death decisions through a network of interactions between anti- and pro-apoptotic members. They include (i) multi-domain proteins, such as Bax or Bak, that are absolutely required for

[1]Team 8 'Cell survival and Tumor Escape in Breast Cancer', UMR 892 INSERM/6299 CNRS/Université de Nantes, Institut de Recherche en Santé de l'Université de Nantes, 8 quai Moncousu, BP 70721, Nantes 1 44007, France; [2]Department of Medical Oncology, Dana-Farber Cancer Institute, Boston, MA 02215, USA; [3]Institut de Cancérologie de l'Ouest (ICO), Centre de Lutte contre le Cancer René Gauducheau, Boulevard Jacques Monod, Saint Herblain-Nantes 44805, France and [4]Plateforme IMPACT Biogenouest, Institut de Recherche en Santé de l'Université de Nantes, 8 quai Moncousu, BP 70721, Nantes 1 44007, France
*Corresponding author: S Barillé-Nion, Team 8 'Cell survival and Tumor Escape in Breast Cancer', UMR 892 INSERM/6299 CNRS/Université de Nantes, Institut de Recherche en Santé de l'Université de Nantes, 8 quai Moncousu, BP 70721, Nantes 44007, France. Tel: +33 0 2 28 08 02 93; Fax: +33 0 2 28 08 02 04; E-mail: sophie.barille@inserm.fr
Abbreviations: BH domain, Bcl-2 homology domain; BRET, bioluminescence resonance energy transfer; Cyto-*c*, cytochrome-*c*; RFP, red fluorescent protein; H2B, histone-2B; MOMP, mitochondrial outer membrane permeabilization; MPM2, mitotic protein monoclonal 2; S62A/D mutants, serine 62 Ala/Asp mutants
Received 16.1.14; revised 28.4.14; accepted 06.5.14; Edited by S Lavandero

MOMP and subsequent cyto-*c* release, (ii) pro-apoptotic BH3-only proteins that are either direct Bax or Bak activators or sensitizer and (iii) anti-apoptotic proteins, such as Bcl-2, Bcl-xL or Mcl-1, that prevent Bax or Bak activation and MOMP.

The balance between the pro- and anti-apoptotic proteins is finely tuned through transcriptional control, various intracellular signalling pathways and post-translational modifications. Alterations in the Bcl-2 network frequently observed in cancer cells are understood to provide a selective advantage by allowing these cells to survive to various stress.[7] As a result, cancer cells may be addicted to this Bcl-2 network for their survival during tumor progression or chemoresistance. In particular, high expression levels of Bcl-2, Bcl-xL or Mcl-1 have been reported in diverse subtypes of breast cancers.[8–10] Their critical role played in survival and chemoresistance defines them as important targets in anticancer therapy, underscoring the therapeutic potential of small molecules BH3 mimetics such as ABT-737[11,12] and its orally analogue ABT-263, that inhibit the anti-apopototic function of Bcl-2, Bcl-xL and Bcl-w or ABT-199 that specifically inhibits Bcl-2.[10] Importantly, cellular dependence on a given Bcl-2 protein ensues from the coexistence of anti-apoptotic signals with a high level of pro-apoptotic potential, creating a mitochondrial state ready for apoptosis, a situation termed 'primed for death'. Primed cells depend on the continuous function of anti-apoptotic proteins to maintain survival. This is the basis for differential clinical response to conventional chemotherapeutic agents that generally kill via the mitochondrial pathway in various cancers.[13,14] This 'primed for death' state can be diagnosed by functional assays using BH3 peptides that can activate Bax or Bak or inhibit Bcl-2 homologues. These assays are particularly useful to uncover the anti-apoptotic barriers mediating resistance developed by cancer cells.

Overexpression of Bcl-2 family homologues, mainly Bcl-2 itself, generally protects cancer cells from mitotic cell death.[4,15] Upon mitotic arrest, these proteins also undergo various post-translational modifications (reviewed in Barillé-Nion *et al.*[16]), whose consequences on cell fates remain uncertain. We hypothesized that such modifications might provide a decisive cue tilting the balance towards cell death. We first sought to define which Bcl-2 homologue was of particular importance for cell survival upon mitotic arrest and whether its anti-apoptotic activity could be eroded during this critical time in proliferating breast cancer cells. We triggered potent mitotic arrest in prometaphase by depleting cells in the anaphase-promoting complex/cyclosome activator Cdc20 or paclitaxel treatment. Our results indicate that mitotic arrest provides a specific priming for mitochondrial apoptotic cell death identifying Bcl-xL as holding a major role in controlling a switch in cell death pathways activated during mitotic arrest from a weak caspase-independent cell death to a strong caspase and Bax/Bak-dependent one. Moreover, our data provide evidence that phosphorylation of Bcl-xL on serine 62 residue that appeared during mitotic arrest, significantly decreased its affinity for Bax, unmasked by ABT-737 treatment and impaired its efficiency in protecting cancer cells from mitotic cell death and yeast from Bax-induced toxicity. Altogether, our results strongly suggest that combining antimitotics with BH3 mimetics targeting Bcl-xL would improve cancer therapy.

Results

Prolonged mitotic arrest prime breast cancer cells for mitochondrial apoptosis regulated by Bcl-xL. In order to obtain a prolonged mitotic arrest in breast cancer cells, we chose to directly target Cdc20 using RNA interference. This led to a potent decrease in Cdc20 mRNA and protein expression (Figure 1a) that was maintained for at least 72 h, as shown at mRNA level (Supplementary Figure 1A). Cdc20 depletion triggered an efficient block of mitosis onset as assessed by flow cytometry analysis after mitotic protein monoclonal 2 (MPM-2) and propidium iodide staining (Supplementary Figure 1B) as soon as 24 h after Cdc20 depletion and at least for 72 h (Figure 1b). During this time, we observed a weak but significantly increased number of dead cells in Cdc20-depleted cells (12% of Annexin V-positive cells compared with control cells). Importantly, this cell death was neither prevented by the pan-caspase inhibitor Q-VD-OPh (Figure 1c) nor by Bax and/or Bak depletion by RNA interference (Figure 6c). Thus, mitotic arrest induced by Cdc20 depletion triggered low and late cell death response in short-term experiments (<72 h). Paclitaxel treatment also induced a potent mitotic arrest but this effect was transient as most of the cells experienced an abnormal mitotic exit without cell division, called mitotic slippage, as soon as 48 h (Figure 1d). Paclitaxel-treated cells for 24 h also exhibited a weak cell death response that was not significantly dependent on caspase activity (Figure 1e). The same results were obtained using the three breast cancer cell lines: MDA-MB-231, MCF-7 and Cal-51 (data shown for MDA-MB-231).

In order to define how breast cancer cells could survive upon mitotic arrest, we first assessed Bcl-2, Bcl-xL and Mcl-1 protein expression by immunoblot analysis in Cdc20-depleted or paclitaxel-treated cells (Supplementary Figures 1C and D). Bcl-2 and Bcl-xL proteins underwent phosphorylation that was sustained over at least 48 h in Cdc20-depleted cells and was transient in paclitaxel-treated cells peaking at 24 h. Mcl-1 expression was not significantly modified during the experiment. We thus performed further experiments at 48 h for Cdc20 depletion and 24 h for paclitaxel treatment. We then analysed whether viable, mitotic arrested cells were primed to apoptotic death using the BH3 profiling assay. The release of cyto-*c* from mitochondria, a direct marker of MOMP, was measured by flow cytometry after incubation with standardized doses of BH3 peptides in cells Cdc20-depleted *versus* control cells. We observed that the main differences in BH3 profiles resided in the significant increase of cyto-*c* loss in Cdc20-depleted cells in response to Puma or Hrk BH3 peptides, but not to the Noxa one (Figure 2). In addition, Bad peptide also tended to trigger more cyto-*c* loss in these cells. The MOMP increase in response to Bad peptide revealed a dependence on either Bcl-2, Bcl-xL or Bcl-w for mitotic survival and in the opposite, the absence of effect of Noxa peptide argued against a role of Mcl-1 in this process. Moreover, the increase of cyto-*c* release in the presence of Hrk peptide that specifically interacts with Bcl-xL strongly supported a major role of Bcl-xL in MOMP regulation in mitotic cells. BH3 profiling performed in viable paclitaxel-treated cells also revealed a trend in increase of cyto-*c* loss when exposed
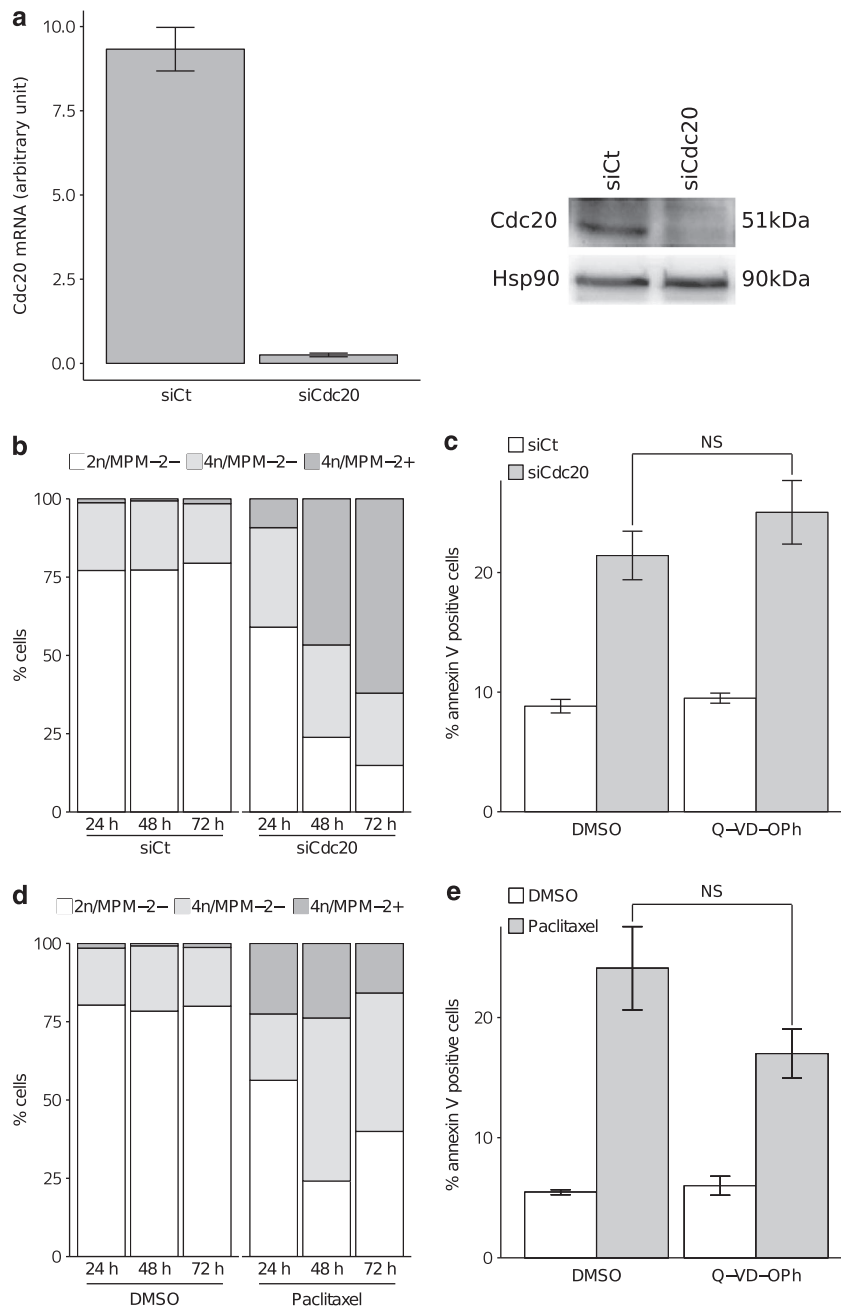
Figure 1 Cdc20 depletion triggered strong mitotic arrest followed by mitochondrial priming alteration, and caspase-independant cell death in breast cancer cells. (**a**) RT-qPCR and immunoblot analysis of Cdc20 expression levels after Cdc20 depletion by RNA interference in MDA-MB-231 cells. MDA-MB-231 cells were transfected with either a control siRNA (siCt) or a Cdc20 siRNA (siCdc20), and the Cdc20 mRNA (upper panel) or the protein (lower panel) levels were analysed using RT-qPCR and immunoblotting, respectively. (**b**) Cell cycle analysis of MDA-MB-231 cells under Cdc20 depletion. MDA-MB-231 cells were transfected with either a control siRNA (siCt) or a Cdc20 siRNA (siCdc20), and harvested at the indicated times. Cells were then stained with propidium iodide (PI) and MPM-2-directed antibody, and analysed by flow cytometry. 2n/MPM-2-negative, 4n/MPM-2-negative, 4n/MPM-2 positive cells corresponding to (G1/S), G2 or post-slippage cells, and mitotic (M) populations, respectively, are indicated. (**c**) Apoptosis analysis of MDA-MB-231 cells after Cdc20 depletion, and treatment or not with Q-VD-OPh, compared with control cells. MDA-MB-231 cells were transfected with either a control siRNA (siCt) or a Cdc20 siRNA (siCdc20), and treated with DMSO or the pan-caspase inhibitor Q-VD-OPh (10 μM). Cells were then stained with Annexin V, and analysed by flow cytometry. (**d**) Cell cycle analysis of MDA-MB-231 cells upon paclitaxel treatment. MDA-MB-231 cells were treated with 70 nM paclitaxel and harvested at the indicated times. Cells were then stained with PI and MPM-2-directed antibody, and analysed by flow cytometry. 2n/MPM-2-negative, 4n/MPM-2-negative, 4n/MPM-2-positive cells corresponding to (G1/S), G2 or post-slippage cells, and mitotic (M) populations, respectively, are indicated. (**e**) Apoptosis analysis of MDA-MB-231 cells after paclitaxel treatment in the presence of Q-VD-OPh or not, compared with control cells. MDA-MB-231 cells were pretreated with DMSO or the pan-caspase inhibitor Q-VD-OPh (10 μM) before paclitaxel treatment (70 nM). Cells were then stained with Annexin V, and analysed by flow cytometry
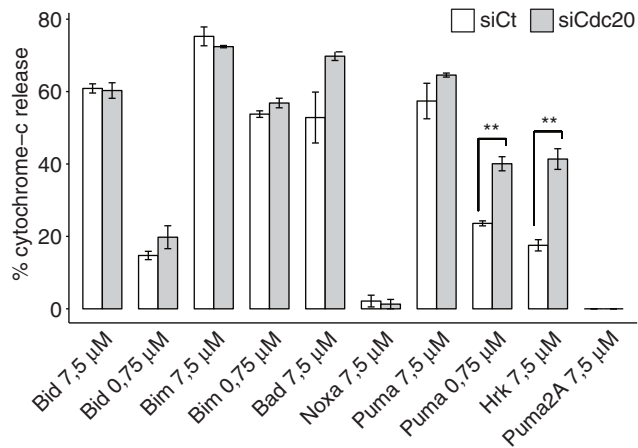
Figure 2 BH3-profiling of MDA-MB-231 cells after Cdc20 depletion compared with control cells. MDA-MB-231 cells were transfected with either a control siRNA (siCt) or a Cdc20 siRNA (siCdc20). After 48 h, cells were harvested, and exposed to the indicated BH3 peptides after permeabilization. Cells were then stained with cyto-*c*-directed antibody, and analysed by flow cytometry. The median fluorescence intensity of cyto-*c* staining obtained after cell exposition to each peptide and measured by flow cytometry was normalized to isotype control and the inert peptide PUMA2A. Data are presented in % of cyto-*c* loss after peptide exposition compared with isotype control

to Bad, Puma or Hrk BH3 peptides as observed upon Cdc20 depletion (Supplementary Figure 2). These results indicate that most of the cells could withstand mitotic arrest for 24–48 h but accumulated an apoptotic signal, which relied at least partially on Bcl-xL.

Bcl-xL protects cells from switching to a strong apoptosis response upon mitotic arrest. We further analysed the specific role of Bcl-xL as the most prominent prosurvival protein during mitotic arrest by sequential depletion of Bcl-xL, Bcl-2 or Mcl-1, and Cdc20 to generate mitotic cells specifically depleted in prosurvival Bcl-2 homologues (Figure 3a). Cdc20 mRNA expression was equally decreased in each experimental setting (data not shown). As shown in Figure 3b, Bcl-xL was the only protein whose depletion triggered extensive cell death in Cdc20-depleted cells. MDA-MB-231 paclitaxel-treated cells were also highly sensitive to Bcl-xL depletion (Figure 3c), as were MCF-7 (Supplementary Figure 3A) or Cal-51 (data not shown) cells. Of note, the pan-caspase inhibitor Q-VD-OPh potently prevented cell death onset in these settings (Figures 3b and c). We then performed a series of single-cell analysis by videomicoscopy using cells expressing a red fluorescent protein (RFP)-tagged histone-2B (H2B) as a marker of chromatin morphology (i.e., chromosome condensation or nuclear fragmentation) and a green fluorescent protein-tagged shRNA construct targeting Bcl-xL to follow cell cycle progression and define kinetic cell response (i.e., mitotic arrest, mitotic slippage, cell death upon paclitaxel treatment) under these conditions. We first observed that in control cells, Bcl-xL depletion triggered a partial cell death response that mostly happened during interphase (Figure 3d). After prolonged mitotic arrest, paclitaxel treatment frequently led to mitotic slippage over the experimental timing. However, Bcl-xL depletion massively shifted the paclitaxel response to

mitotic cell death. Indeed, as depicted in Figure 3d, the majority of cells (68%) died rapidly after entry into mitosis (Figure 3e). These results underlined the extreme sensitivity of Bcl-xL-depleted cells to death during abnormal mitosis onset.

Importantly and according to the effects of Bcl-xL depletion by RNA interference, the bivalent Bcl-2/Bcl-xL inhibitor, ABT-737 that had no significant effect on cells when used as single agent, triggered strong mitotic cell death (60%) when combined with paclitaxel in single-cell analysis by videomicroscopy (Figures 4a and b) or in cell death assays performed in MDA-MB-231 (Figure 6a) or in MCF-7 cells (Supplementary Figure 3B, left panel). This was also observed in Cdc20-depleted cells, as shown in end-point analysis in MCF-7 cells (Supplementary Figure 3B, right panel). Interestingly, the orally bivalent Bcl-2/Bcl-xL inhibitor ABT-263 also led to synergistic cell death when combined with paclitaxel, in contrast to the specific Bcl-2 inhibitor ABT-199 used in the three breast cancer cell lines tested (Supplementary Figure 3C and data not shown). This underlined again the specific Bcl-xL dependence of these cancer cells during mitotic arrest.

We further asked whether Bcl-xL could protect cells from mitotic cell death upon paclitaxel treatment using Bcl-xL-overexpressing cells (Figure 5a). By videomicroscopy analysis, we could not detect any significant cell death upon paclitaxel treatment in Bcl-xL-overexpressing MCF-7 cells in comparison to control MCF-7 cells (Figures 5b and c). Indeed, most Bcl-xL-overexpressing cells experienced mitotic slippage upon prolonged paclitaxel treatment and more than 90% of cells were still alive at the end of the experiment. Thus, Bcl-xL overexpression strongly protected mitotic arrested cells from mitotic death and allowed mitotic slippage to occur.

The shift in the mitotic response controlled by Bcl-xL involved Bax and was modulated by Bcl-xL phosphorylation on serine 62. We first observed that caspase inhibition obtained using the pan-caspase inhibitor, Q-VD-OPh, completely abrogated mitotic cell death when Bcl-xL was targeted in MDA-MB-231 and MCF-7 cells (Figure 6a, Figures 3b and c, Supplementary Figure 3B). In addition, as BH3 profiling argued for the implication of mitochondria in mitotic cell death, we explored whether the pro-apoptotic Bax and/or Bak were required for triggering this process. Bax and Bak were first depleted in cells by RNA interference (Figure 6b) before subsequent depletion of Cdc20 or paclitaxel treatment. Our results indicated that eventhough Bax and/or Bak were not necessary for cell death occurring upon Cdc20-depletion alone, Bax was required for the onset of apoptosis when Cdc20 depletion was combined to Bcl-xL inhibition using ABT-737 (Figure 6c). Regarding paclitaxel-induced mitotic arrest, Bax depletion was more effective in protecting mitotic cell death than Bak depletion, but a Bax/Bak cooperation could be detected (Figure 6d), suggesting possible Bak involvement in death signalling occurring in some cells that might slipped out after 24-h treatment with paclitaxel.

As Bcl-xL phosphorylation on S62 has been previously observed during mitotic arrest, we then focused our attention on this residue to define whether this post-translational Bcl-xL
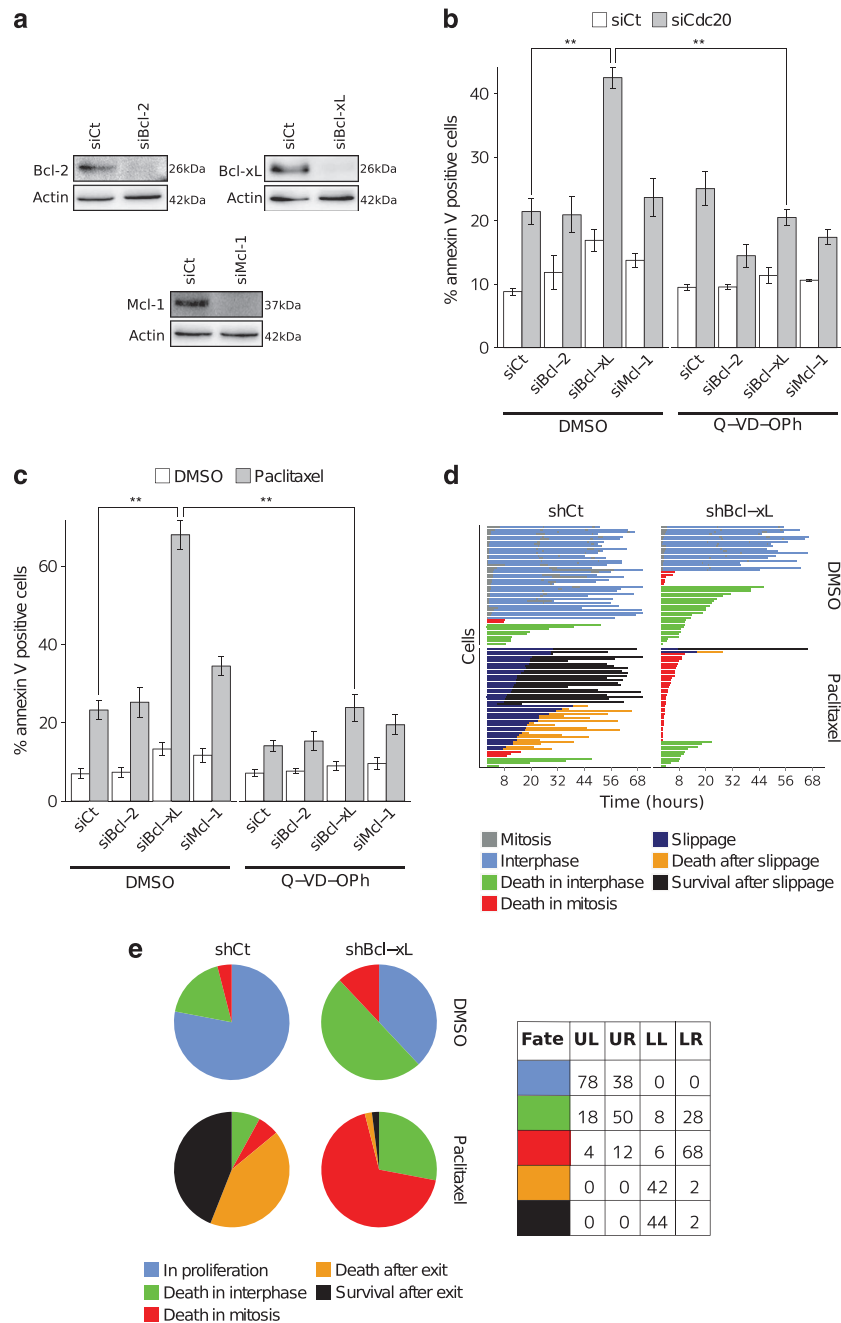
a

b

c

d

e

Fate	UL	UR	LL	LR
	78	38	0	0
	18	50	8	28
	4	12	6	68
	0	0	42	2
	0	0	44	2

Figure 3 Bcl-xL but not Bcl-2 or Mcl-1 depletion sensitized breast cancer cells to cell death. (**a**) Immunoblot analysis of Bcl-2, Bcl-xL and Mcl-1 expression levels after their depletion by RNA interference in MDA-MB-231 cells. MDA-MB-231 cells were transfected, respectively, with control, Bcl-2, Bcl-xL and Mcl-1 siRNA. The expression levels of Bcl-2, Bcl-xL and Mcl-1 were then evaluated by immunoblot analysis. (**b**) Apoptosis analysis of MDA-MB-231 cells after Bcl-2, Bcl-xL or Mcl-1 depletion, and Cdc20 depletion, in the presence of the pan-caspase inhibitor Q-VD-OPh or not. MDA-MB-231 cells were transfected, respectively, with control (siCt), Bcl-2 (siBcl-2), Bcl-xL(siBcl-xL) and Mcl-1 (siMcl-1) siRNA, and 24 h later transfected with either control siRNA (siCt) or Cdc20 siRNA (siCdc20) in presence of Q-VD-OPh (1O μM) or not. Cells were finally stained with Annexin-V, and analysed by flow cytometry. (**c**) Apoptosis analysis of MDA-MB-231 cells after Bcl-2, Bcl-xL or Mcl-1 depletion, before treatment with paclitaxel and Q-VD-OPh or not. MDA-MB-231 cells were transfected, respectively, with control (siCt), Bcl-2 (siBcl-2), Bcl-xL (siBcl-xL) and Mcl-1 (siMcl-1) siRNA, and 24 h later, cells were treated or not with paclitaxel and/or Q-VD-O-Ph for 24 h. Cells were finally stained with Annexin V, and analysed by flow cytometry. (**d**) Fate profiles of MDA-MB-231 cells expressing either control or Bcl-xL shRNA, and treated or not with paclitaxel. MDA-MB-231 cells coding for RFP-H2B were transduced with lentivectors coding for control shRNA (shCt) or shRNA-targeting Bcl-xL (shBcl-xL). After 48 h, cells were synchronized using a double thymidine block, treated with either DMSO or paclitaxel (70 nM), and finally monitored by time-lapse microscopy during 72 h. Data for 50 cells per condition are presented with each horizontal line representing a single cell, the colour of the line indicating the fate according to the legend and the length of the line indicating the duration of the observed fate. Time 0 represents the time of addition of paclitaxel. (**e**) End-point cell fates of MDA-MB-231 cells expressing either control or Bcl-xL shRNA, and treated or not with paclitaxel. The proportion of each fate at the end point of experiments (72 h) derived from data presented in **d** are shown in pie charts and % of cell fates in the associated table (UL = upper left, UR = upper right, LL = lower left and LR = lower right, corresponding panels in **d**)
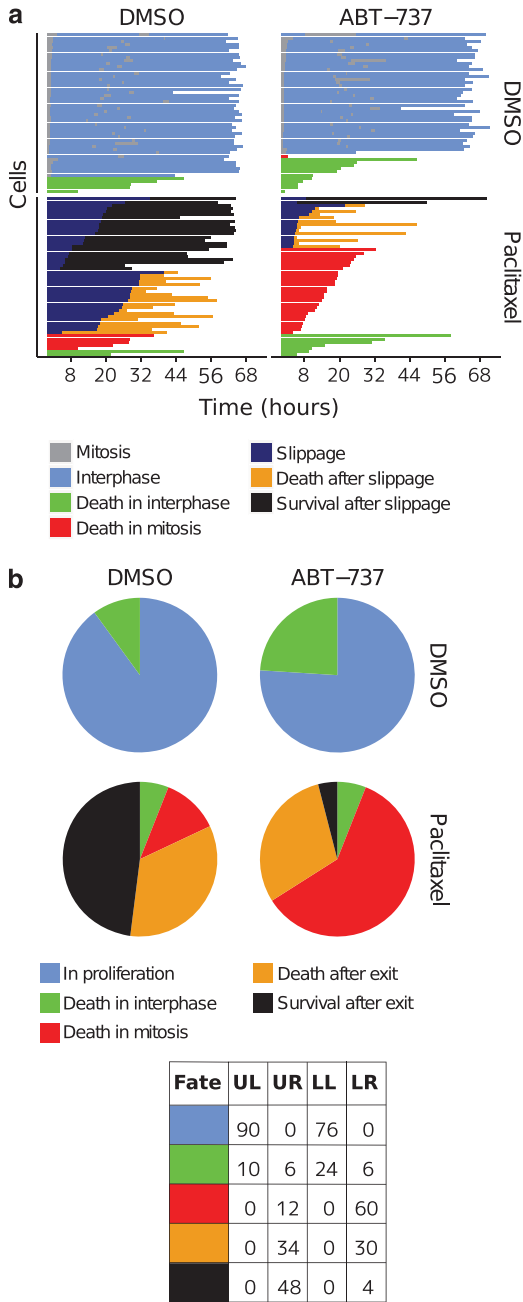
a

■ Mitosis (grey)	■ Slippage (dark blue)
■ Interphase (light blue)	■ Death after slippage (orange)
■ Death in interphase (green)	■ Survival after slippage (black)
■ Death in mitosis (red)	

b

■ In proliferation	■ Death after exit
■ Death in interphase	■ Survival after exit
■ Death in mitosis	

Fate	UL	UR	LL	LR
(blue)	90	0	76	0
(green)	10	6	24	6
(red)	0	12	0	60
(orange)	0	34	0	30
(black)	0	48	0	4

Figure 4 ABT-737 treatment induced mitotic cell death under mitotic arrest. (**a**) Fate profiles of MDA-MB-231 cells treated with either DMSO or ABT-737, and treated or not with paclitaxel. MDA-MB-231 cells were infected with H2B-RFP-coding lentivectors and treated with either DMSO or ABT-737 (1 μM). Cells were then synchronized using a double thymidine block, treated with either DMSO or paclitaxel (70 nM), and finally analyse by time-lapse videomicrocopy during 72 h. Data for 50 cells per condition are presented. Time 0 represents the time of addition of paclitaxel. (**b**) End-point cell fates of MDA-MB-231 cells treated or not with paclitaxel and ABT-737. The proportion of each fate at the end point of experiments (72 h) derived from data presented in Figure 5a are shown in pie charts and % of cell fates in the associated table (UL = upper left, UR = upper right, LL = lower left and LR = lower right, corresponding panels in **a**)

modification could modulate Bcl-xL function in mitotic response. We indeed observed specific phosphorylation on S62 upon Cdc20 depletion or paclitaxel treatment (Figure 7a).

Importantly, using phospho-mimetic (S62D-Bcl-xL) or phospho-deficient (S62A-Bcl-xL) Bcl-xL mutants whose ectopic expression levels in cells were comparable (Figure 7b), we evidenced that S62 residue on Bcl-xL controlled anti-apoptotic function of Bcl-xL upon mitotic arrest combined with ABT-737 treatment. Indeed, in contrast to overexpression of S62A-Bcl-xL mutant in mitotic cells, S62D-Bcl-xL mutant expression did not prevent these cells from cell death under these conditions (Figure 7c). Interestingly, using a yeast model in which Bax expression led to strong growth inhibition, we observed that the S62D mutant was less effective to protect yeast from growth inhibition than was the S62A mutant (when equally expressed; Supplementary Figure 4A). These results are consistent with the effect observed in mammalian cells and, in addition, they highlighted a differential ability of Bcl-xL mutants in neutralizing Bax activity.

We then directly analysed whether the S62 phosphorylation modulates the interactions that Bcl-xL can engage with its partner Bax, which functions as a major effector of mitotic cell death upon Bcl-xL inhibition. To this end, we used a bioluminescence approach based on the measurement of energy transfer (BRET) between N-terminal Luciferase-fused Bax and N-terminal eYFP-fused S62-Bcl-xL variants. Of note, both eYFP-Bcl-xL mutants localized to the mitochondrial membrane as wild-type Bcl-xL did (Supplementary Figure S5A), indicating that the introduced mutation does not affect subcellular localization. As shown in Figure 8a, both eYFP-fused S62D or S62A-Bcl-xL mutants interacted with Luciferase-fused Bax and produced BRET signals in a saturable manner. Moreover, as expected, treatment of cells with ABT-737 (1 μM) significantly decreased BRET signals observed with either mutant. However, the $BRET_{50}$ values (calculated as indicated in Supplementary Figure S5B) were lower in case of S62A-eYFP-Bcl-xL than for the S62D-eYFP-Bcl-xL, indicating higher relative affinity between Bax and S62A variant than the S62D one (Figure 8b). Moreover, ABT-737 treatment clearly evidenced the decreased relative affinity of S62D-Bcl-xL mutant for Bax compared with the S62A one. In addition, when we performed dose–response analysis, we found that the IC_{50} of ABT-737 required for disrupting Bcl-xL from Bax was lower in S62D-Bcl-xL/Bax complexes ($IC_{50} = 20.2 \pm 1.9$ nM) than in those formed with S62A-Bcl-xL mutants ($IC_{50} = 38.7 \pm 2.9$ nM; Figure 8c). Using a yeast assay, we also observed that ABT-737 (that was inactive on the S62A-Bcl-xL or S62D-Bcl-xL expressing control yeasts) was significantly more toxic in S62D-Bcl-xL-transformed than in S62A-Bcl-xL-transformed Bax-expressing yeasts (Supplementary Figure 4B). Altogether, these results argue that phosphorylation of serine 62 in Bcl-xL weakens its interaction with Bax and enhances its sensitivity to pharmacological inhibition.

Discussion

Enhancing efficacy of antimitotic agents and unravelling the specific network that governs the delicate balance between death and survival during mitotic cells is now critical in anticancer treatment. There is indeed a need to understand how cell death pathways interconnect during mitotic arrest, and whether and how pharmacologically tractable Bcl-2 family
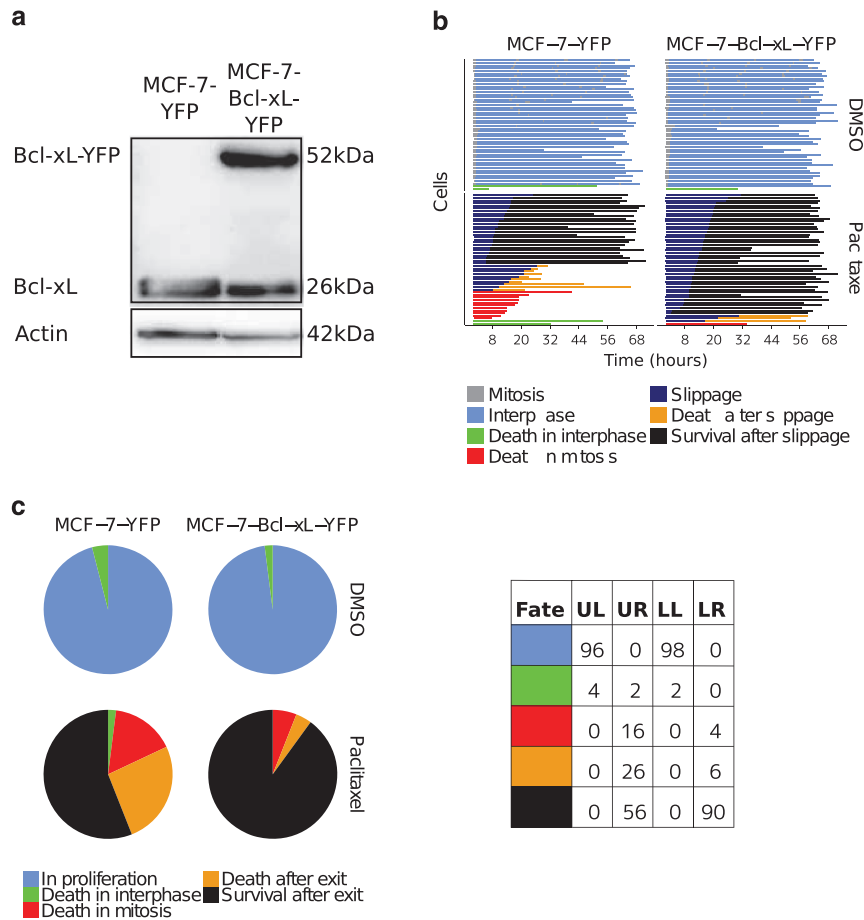
a

b

Mitosis	Slippage
Interp ase	Deat a ter s ppage
Death in interphase	Survival after slippage
Deat n m tos s	

c

Fate	UL	UR	LL	LR
	96	0	98	0
	4	2	2	0
	0	16	0	4
	0	26	0	6
	0	56	0	90

In proliferation	Death after exit
Death in interphase	Survival after exit
Death in mitosis	

Figure 5 Bcl-xL overexpression protected cells from mitotic cell death. (**a**) Immunoblot analysis of Bcl-xL expression in MCF-7-YFP and MCF-7-Bcl-xL-YFP cells. (**b**) Fate profiles of MCF-7 cells expressing either YFP or Bcl-xL-YFP, and treated or not with paclitaxel. MCF-7-YFP and MCF-7-Bcl-xL-YFP cells were infected with H2B-RFP-coding lentivectors. Cells were then synchronized using a double thymidine block, treated with either DMSO or paclitaxel (70 nM), and finally analysed by time-lapse videomicrocopy during 72 h. Data for 50 cells per condition are presented. (**c**) End-point cell fates of MCF-7 cells expressing either YFP or Bcl-xL-YFP, and treated or paclitaxel. The proportion of each fate at the end point of experiments (72 h) derived from data presented in Figure 4b are shown in pie charts and % of cell fates in the associated table (UL = upper-left, UR = upper-right, LL = lower-left and LR = lower-right, corresponding panels in **b**)

members control one or more of these pathways. In this report, using cellular functional assays, we have emphasized the prominent role of Bcl-xL in maintaining cell survival in mitotic arrest obtained by both Cdc20 depletion and paclitaxel treatment. In fact, using BH3 profiling and videomicroscopy, we describe a genuine switch in cell death pathways triggered during metaphase-arrested cells that mainly depends on Bcl-xL. Indeed, mitotic cells underwent extensive apoptosis when Bcl-xL was depleted or pharmacallogically targeted by the BH3 mimetic ABT-737, whereas they were able to sustain a prolonged mitotic arrest when Bcl-xL was functional. In addition, we evidenced that Bcl-xL phosphorylation on Ser62 residue by mitotic kinases directly affected both its prosurvival function and its affinity for Bax leading to a Bax-dependent cell death using BRET assay in whole cells and survival assays based on cancer cells and yeast models.

Our results demonstrate that cancer cells experiencing a prolonged mitotic arrest were able to maintain survival pathways, in particular in Cdc20-depleted cells that exhibited a few propense to slip out mitotic arrest in contrast to paclitaxel-treated cells. In the weak fraction of mitotic cells that

die, the cell death does not rely on canonical pathways (i.e., caspase- and Bax/Bak-dependent). This is consistent with what has been previously observed,[17] especially when cells contain high levels of Bcl-2 homologues.[4,5] However, we show for the first time that mitotic arrest triggers in cells a specific apoptotic priming compared with asynchronous cells. Indeed, based on the BH3 profiling assay relying on mitochondrial response to peptides derived from BH3 domains,[14] we observed that an increase in sensitivity to Puma, Hrk and Bad BH3 peptides, as measured by an increase in cyto-*c* release, could be specifically detected in mitotic cells. As these three peptides share their capacity to interact with and inhibit Bcl-xL, among prosurvival Bcl-2 homologues (especially Hrk peptide that essentially interacts with Bcl-xL) these results strongly suggest that a specific dependence on the prosurvival activity of this protein installs during mitotic arrest. Highly consistent with this, Bcl-xL was the only anti-apoptotic Bcl-2 homologue whose depletion potently induced death in mitotically arrested cells. Importantly, single-cell analysis by videomicroscopy clearly demonstrated that a vast majority of Bcl-xL-depleted cells
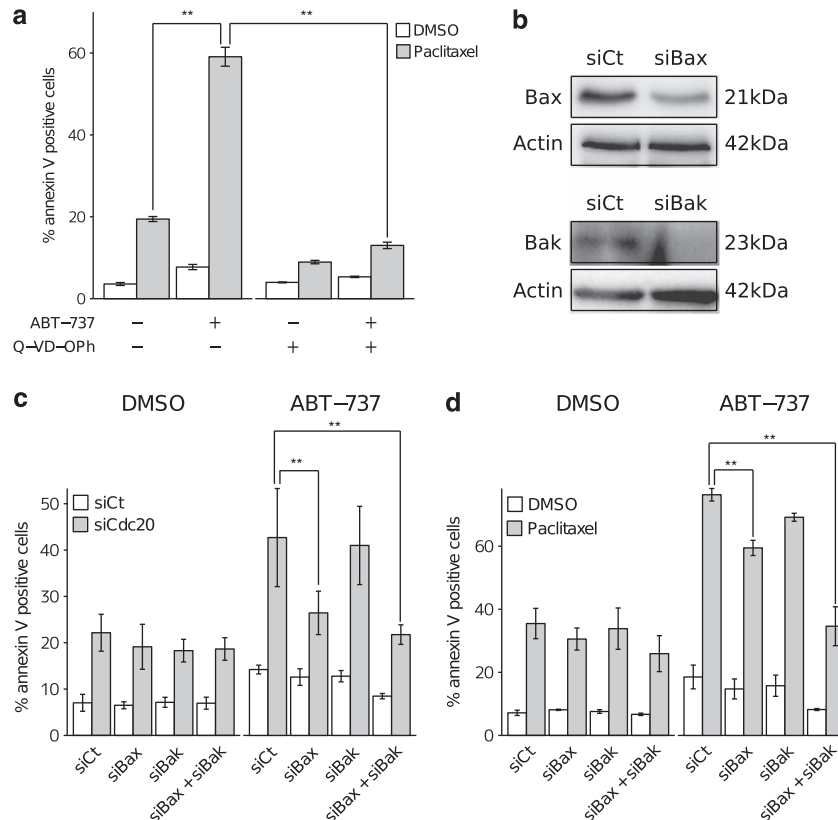
Figure 6 Bax is required for cell death induced by Bcl-xL depletion under prolonged mitotic arrest. (**a**) Apoptosis analysis of MDA-MB-231 cells after Cdc20 depletion and ABT-737 treatment. MDA-MB-231 cells were transfected, respectively, with either control or Cdc20 siRNA. After 24 h, cells were treated with DMSO or Q-VD-OPh for 48 h. Cells were finally stained with Annexin V, and analysed by flow cytometry. (**b**) Immunoblot analysis of Bax and Bak expression levels after depletion of these proteins by RNA interference in MDA-MB-231 cells. MDA-MB-231 cells were transfected, respectively, with control (siCt), Bax (siBax) and Bak (siBak) siRNA. The expression levels of Bax and Bak were evaluated after 48 h by immunoblot analysis. (**c**) Apoptosis analysis of MDA-MB-231 cells after Bax, Bak or Bax + Bak depletion, and depletion or not of Cdc20, compared with control cells. MDA-MB-231 cells were first transfected, respectively, with control (siCt), Bax (siBax), Bak (siBak) and Bax and Bak (siBax + siBak) siRNA, and then transfected with either control siRNA (siCt) or Cdc20 siRNA (siCdc20). Cells were finally stained with Annexin V, and analysed by flow cytometry. (**d**) Apoptosis analysis of MDA-MB-231 cells after Bax, Bak or Bax and Bak depletion, and treatment or not with paclitaxel, compared with control cells. MDA-MB-231 cells were transfected, respectively, with control, Bax, Bak or Bax and Bak siRNA, and then treated with either DMSO or paclitaxel (70 nM) for 48 h. Cells were finally stained with Annexin V, and analysed by flow cytometry

underwent rapid apoptosis when they enter into mitosis compared with control cells that either survive in a mitotic arrested state or after abnormal mitotic exit or die during interphase upon paclitaxel treatment, indicating that Bcl-xL is specifically required, under these conditions, for maintaining survival during prolonged mitosis. In the opposite, Bcl-xL overexpression completely blunt mitotic cell death, thus allowing mitotic slippage to happen. Of note, this experiment indicates that maintaining survival during mitotic arrest facilitates mitotic slippage in cancer cells and the generation of polyploid cells, potentially dangerous because of their chromosome instability.[2]

Interestingly, mitotic cell death related to Bcl-xL depletion could also be triggered using ABT-737 or ABT-263, both potent inhibitors of Bcl-2/Bcl-xL.[11,12] In line with this, cell death triggering in various epithelial cell lines[18,19] and tumor response in human breast basal-like tumor xenografts[8] were significantly improved in therapy combining ABT-737 or ABT-263 and taxanes. This is mostly consistent with the BH3 profiling assays and it suggests that the ability of Bcl-xL to regulate cell survival during mitotic arrest relies on

its BH3-binding activity and can be harnessed pharmaceutically. In contrast, ABT-199 combined to paclitaxel did not increase cell death in these cells compared with paclitaxel alone. This strongly argues for a prominent role of Bcl-xL over Bcl-2 in mitotic arrested breast cancer cells. This contrasts with previous reports that evidenced Bcl-2 capacity to counteract mitotic cell death but that investigated the role of Bcl-2 when it was ectopically overexpressed in cell lines.[4,15] Bcl-2 contribution in antimitotic-induced cell death cannot be excluded, as ABT-737 treatment in breast tumors with high expression of this protein sensitized cancer cells to doxetaxel treatment.[10] In our hands, endogenous Mcl-1 did not contribute to mitotic survival, eventhough its lability during mitotic arrest has been incriminated in sensitivity to antimitotic agents.[20] This strengthens the notion that Mcl-1 may not regulate survival as stringently as Bcl-xL in cancer cells treated by antimitotic agents, as this was already observed in cells treated with topoisomerase inhibitors.[9]

We further demonstrated that cell death occurring during mitotic arrest upon Bcl-xL depletion or inhibition was dependent on caspase activation and Bax or Bax/Bak
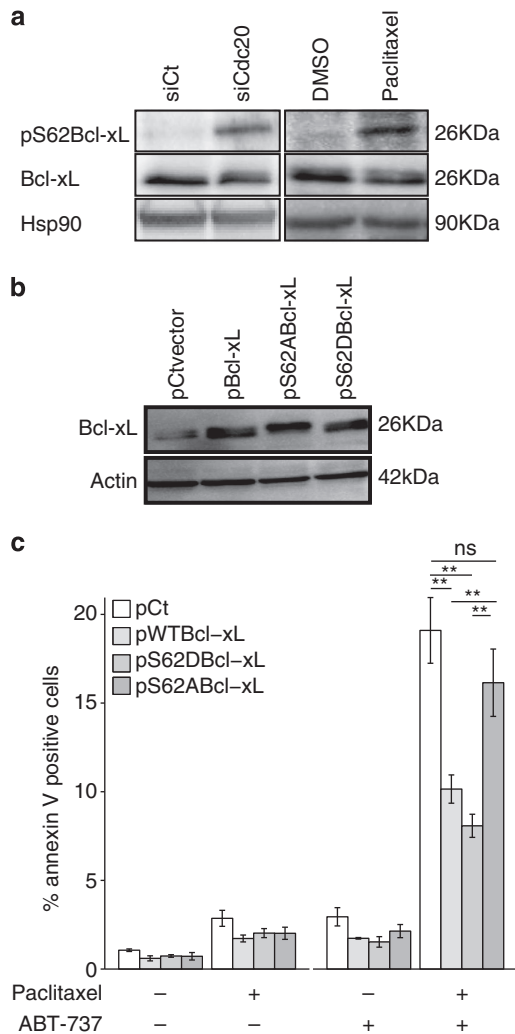
Figure 7 Serine 62 phosphorylation of Bcl-xL occurring during prolonged mitotic arrest, promoted mitotic cell apoptosis. (**a**) Immunoblot analysis of S62 phosphorylation of Bcl-xL (pS62Bcl-xL) expression levels after Cdc20 depletion or paclitaxel treatment. MDA-MB-231 cells were transfected with either control or Cdc20 siRNA for 48 h or treated with paclitaxel for 12 h, harvested and the expression level of pS62Bcl-xL were finally evaluated by immunoblot analysis with S62-phospho-specific or total Bcl-xL antibodies. (**b**) Immunoblot analysis of Bcl-xL mutants. MDA-MB-231 cells were transfected with plasmids coding for wt Bcl-xL or S62(A or D)Bcl-xL mutants and analysed by immunoblotting 48 h later. (**c**) Apoptosis analysis of MDA-MB-231 cells after Bcl-xL or its S62 mutants (S62A- or S62D-Bcl-xL) overexpression, and treatment or not with paclitaxel and ABT-737, compared with control cells. MDA-MB-231 cells were transfected, respectively, with control plasmid (pCt), plasmids coding for Bcl-xL (pBcl-xL) or its S62(A or D) mutants (pS62(A or D)Bcl-xL). Cells were then treated with either DMSO or paclitaxel (70 nM), and finally stained with Annexin-V, and analysed by flow cytometry

cooperation. One hallmark of mitotic arrest is prolonged activity of various kinases including cyclin-dependent kinase 1, Aurora, Polo-like or Jun kinases, which coordinate the phosphorylation cascade of various substrates, among them Bcl-2, Bcl-xL and Mcl-1.[21–25] A recent report highlighted mitotic Bcl-xL phosphorylation and proposed to include its evaluation to define a mitotic death signature.[26] We show here that Bcl-xL was indeed phosphorylated on its Ser62 residue upon mitotic arrest. This phosphorylation site stands within

the non-structural loop that links the BH3 and BH4 domains of the protein,[27] but is not directly part of the BH3-binding site that mediates interactions with BH3-only proteins. Using Ser62 Bcl-xL mutants, we first observed that the phosphodefective S62A Bcl-xL mutant significantly protected cancer cells from death during mitotic arrest combined to ABT-737 treatment, whereas the phosphomimetic S62D mutant did not, as also reported by Terrano et al.[21] It strongly suggests that mitotic phosphorylation of Bcl-xL erodes its anti-apoptotic activity and that this event represents a key element in cell fates occurring upon antimitotic treatments.

As the observed cell death was Bax dependent, we first evidenced the ability of Bcl-xL mutants to protect cells from a Bax-induced growth inhibition in a yeast assay.[28] We then used an approach based on BRET assays to quantify the interactions between Bax and S62-Bcl-xL mutants in a whole-cell context. We observed that S62D-Bcl-xL/Bax complexes were particularly sensitive to disruption by ABT-737 compared with the phosphodefective Bcl-xL mutant, as they were in the Bax-induced growth inhibition in yeast assays. This coincides with the previous observation that S62A-Bcl-xL mutant was more competent to bind Bax than the S62D mutant using co-immunoprecipitation experiments.[22] We thus speculate that phosphorylation in the flexible loop of Bcl-xL alters its overall folding in such a way that ABT-737 would impact on its BH3-binding activity allosterically. Phosphorylation of Bcl-xL may be thus a key event in mitotic cell death upon antimitotic treatment because it disables Bcl-xL/Bax complexes, an event that constitutes in itself a death signal.[28]

In addition, a recent report proposes that Bcl-xL inhibits and maintains Bax in the cytosol by constant retrotranslocation of mitochondrial Bax,[29] but we do not know yet how Bcl-xL phosphorylation might impact this capacity. A competitive displacement of Bim from anti-apoptotic proteins may also takes place.[30] However, as massive apoptosis is observed in Bcl-xL-depleted cells upon mitotic arrest, other, Bcl-xL-independent, death signals must be involved. What these signals are is currently under investigation in our laboratory.

Overall, our work highlights that upon antimitotic treatment, a fine balance between pathways that control cell death and mitotic slippage will finally govern cell fates. As Bcl-xL critically regulates cell death upon mitotic arrest, inhibitors of its anti-apoptotic activity could be particularly effective in enhancing mitotic death and in limiting cancer cells often having a leaky mitotic checkpoint to escape mitotic arrest. Comprehensive research on mitosis has considerably increased our understanding of why cell responses to antimitotic drugs are variable. Our data, plus preclinical data that revealed that combining antimitotic drugs with BH3-mimetics strongly accelerates apoptosis during mitotic arrest,[18] point to exciting potential for the treatment of cancer.

Materials and Methods

Cell culture. The breast cell lines MDA-MB-231 and MCF-7 were obtained from the American Type Culture Collection (Rockville, MD, USA) and were maintained in DMEM supplemented with 5% fetal bovine serum (FBS), 2 mM glutamine (Gibco, Saint Aubin, France), 50 U/ml penicillin and 50 ng/ml streptomycin (Gibco). In the case of MCF-7-YFP or MCF-7-YFP-Bcl-xL cells, which have been transfected with peYFP-C1 control plasmid (Clontech), or peYFP-Bcl-xL coding for N-terminal-YFP-tagged Bcl-XL (YFP-Bcl-xL), respectively, selection agent G418 (1 mg/ml) was added to culture media.
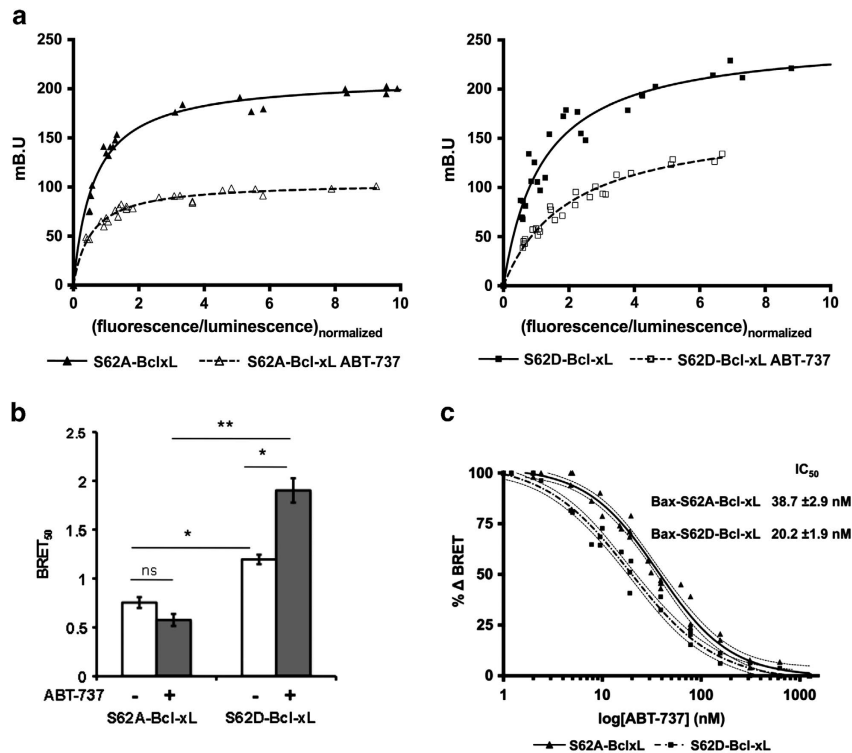
Figure 8 Quantitative BRET analysis indicated that serine 62 phosphorylation of Bcl-xL weakened Bax/Bcl-xL interactions upon ABT-737 treatment. (**a**) Donor saturation assay analysis: saturation curves were performed on MCF-7 cells using increasing amount of vectors encoding S62A- or S62D-YFP-Bcl-xL (triangle and square, respectively) in the presence of a fixed amount of the vector-encoding Rluc-Bax in the presence (full symbol and line) or not (empty symbol and dashed line) of ABT-737 (1 μM). BRET ratios (mB.U, milliBRET Unit) are measured for every YFP-Bcl-xL plasmid concentrations and are plotted as a function of the ratio of total acceptor to donor fluorescence (YFP-Bcl-xL/Rluc-Bax, normalized on the ratio obtained for 100 ng YFP-Bcl-xL). The data were fitted using a nonlinear regression equation assuming a single binding site. Data shown represent results from one of three separate BRET titration experiments (performed in duplicate) that produced quantitatively similar results. (**b**) BRET$_{50}$ for S62A- or S62D-YFP-Bcl-xL/Rluc-Bax treated or not with ABT-737 (1 μM) was calculated from the saturation curves showed in the Supplementary Figure 2. (**c**) Dose–response effect of ABT-737 on disruption of S62A- or S62D-Bcl-xL/Rluc-Bax complexes. MCF-7 cells were transiently transfected with a constant amount of plasmid DNA encoding the donor Rluc-Bax (50 ng) and plasmid DNA encoding the acceptor S62A- or S62D-YFP-Bcl-xL (200 ng), treated or not with increasing dose of ABT-737 (1 to 1000 nM). %ΔBRET is plotted as a function of the semi-logarithmic ABT-737 concentrations. The data were fitted using a nonlinear regression, which provided the IC$_{50}$, the concentration of ABT-737 inhibitor where the BRET signal for a fixed ratio response is reduced by half

Reagents and transfection. The BH3-mimetics ABT-737, ABT-263 and ABT-199 were purchased from Selleck Chemicals (Houston, TX, USA), the pan-caspase inhibitor Q-VD-OPh from R&D Systems (Abingdon, UK) and paclitaxel from Sigma-Aldrich (Saint-Quentin Yvelines, France).

RNA interference was performed either by transfection using Lipofectamine RNAiMax (Invitrogen, Saint-Aubin, France), according to the manufacturer's instructions, or by lentiviral transduction as previously described.[31] The following siRNAs were used: control siRNA (D-001810) and siRNA Bak (L-003305), siRNA Bcl-xL (L-003458) from Dharmacon (Lafayette, CO, USA), siRNA Cdc20 (4392420) from Life Technologies (Saint Aubin, France), siRNA Bcl-2 (sc-29214) from Santa Cruz Biotechnology (Bergheimer, Germany), siRNA Mcl-1 (120644) from Ambion (Saint Aubin, France), siRNA Bax from IDT (Leuven, Belgium). The following siRNA sequence was used in lentiviral experiments targeting Bcl-xL: 5′-AGGATA-CAGCTGGAGTCAG-3′.

Plasmid transfection was made by using Lipofectamine 2000 (Invitrogen), according to the manufacturer's instructions and medium was changed 6 h later.

The lentivector coding for Histone-2B-RFP was kindly provided by Jan Van Deursen, Mayo Clinic, Rochester, MN, USA.

FACS-based cell death assays. For the detection of apoptosis, floating and adherent cells were harvested and analysed by flow cytometry using the Annexin-V-binding assay (Beckman Coulter, Villepinte, France), according to the manufacturer's instructions. Flow-cytometry analysis was performed on a FACSCalibur by using the CellQuestPro software in the Flow Cytometry Facility, CytoCell, SFR Bonamy, INSERM, Nantes, France. For RNA interference, cells were first transfected with siRNA-targeting Cdc-20, Bcl-2, Bcl-xL, Mcl-1, Bax or

Bak; 24 h later, cells were treated or not for 24 h with ABT-737 (1 μM), paclitaxel (70 nM) and/or Q-VD-Oph (10 μM added 1 h prior further treatment), depending on experiments. For Bcl-xL overexpression, cells were first transfected with pcDNA3 control or pcDNA3 coding for Bcl-xL wt or Ser62 A/D mutants; 48 h later, cells were treated by paclitaxel and/or ABT-737 for 24 h before cell death analysis.

Cell cycle assay. Cells were analysed by two-dimensional flow cytometry using MPM-2 as a mitotic marker and propidium iodide. Cells were transfected with control or Cdc20-directed siRNA, or treated with paclitaxel (70 nM) and were then harvested 24, 48 and 72 h after transfection or treatment. Samples were fixed overnight in 12.5%PBS-FBS–50% ethanol solution, washed and stained 1 h at 4 °C with MPM-2-FITC (16–155, 1 : 800, Millipore, Molsheim, France) antibody as recommended by the manufacturer. Flow-cytometry analysis was performed on a FACSCalibur.

BH3 profiling assay. Cells were transfected with control or Cdc20-directed siRNA, or treated with paclitaxel (70 nM), harvested after 48 h and intracellular–stain BH3 profiling (iBH3) was performed.[32,33] Cells were suspended in DTEB and added to peptides in DTEB/0.002% digitonin (w/v) to permeabilize cells and expose mitochondria to peptides for 60 min at 25 °C. Fixation for 15 min with 2% formaldehyde terminated peptide exposure, and formaldehyde was neutralized by the addition of 400 mM glycine/570 mM Tris-HCl pH 9.1 for 15 min. Staining for cyto-c (Clone 6H2.B4, BD Bioscience, San Jose, CA, USA) was performed by addition of saponin, FBS and BSA to a final concentration of 0.1%, 2%, and 1% (w/v), respectively, followed by storage overnight at 4 °C. The median fluorescence intensity (MFI) of the cyto-c staining was normalized to isotype

control and inert peptide (PUMA2A) controls. The percentage of cyto-*c* release was calculated as following: % cyto-*c* release = 100-[MFI(Sample)-MFI(Isotype)]/ [MFI(PUMA2A)-MFI(Isotype)] × 100.

Single-cell videomicroscopy. MDA-MB-231, MCF-7-eYFP and MCF-7-eYFP-Bcl-xL cells were infected with H2B-RFP lentivectors (MOI = 3), washed 6 h later and grown during 48 h. Cells were then harvested and seeded in 24-well plates at 3×10^4 cells per well. A double thymidine block (0.626 M) of 24 h separated by a 16-h release was applied before analysis. When applicable, shCt or shBcl-xL lentivectors were added for 48 h before the double block thymidine was made. Finally, cells were released 1 h before addition of drugs and analysis. Imaging was performed using a Leica DMI 4000 Bioimager (Leica, Nanterre, France) with the Metamorph in the MicroPIcell imaging facility (SFR Bonamy, FED4203/Inserm UMS 016/CNRS 3556, Nantes, France). Images were collected every 10 min using a × 10 objective. Image sequences were viewed using NIH ImageJ software, and cell behavior was analysed manually.

Immunoblotting. Protein extracts were obtained after cell lysis at 4 °C in buffer containing 50 mM Tris-HCl, pH 8.1, 1% SDS, 10 mM EDTA, 1 mM PMSF, 10 μg/ml aprotinin, 10 μg/ml leupeptin, 10 μg/ml pepstatin, 1 mM Na3VO4, 50 mM NaF and sonication. SDS-PAGE were run on 12.5% polyacrylamide gel and proteins transferred to a PVDF membrane. The following antibodies were used at the indicated dilution: Bcl-2 (MO887, 1 : 500, Dako, Hamburg, Germany), Bcl-xL (1018-1, 1 : 1000, Epitomics, Burlingame, CA, USA), Mcl-1 (sc-819, 1 : 500, Santa Cruz Biotechnology, Heidelberg, Germany), Bax (A3533, 1 : 500, Dako), Bak (556396, 1 : 500, BD Pharmingen, Heidelberg, Germany), Bcl-xL pS62-phospho-specific antibody (AB3573, 1 : 500, Chemicon Biosciences, Le Pont de Claix, France), Cdc20 (#4823, 1 : 500, Cell Signaling, Molsheim, France). Incubation of antibodies was made in a solution of 0.1% TBS-Tween-20– 1%BSA at 4 °C overnight. Membranes were finally washed and incubated 1 h with peroxidase-conjugated secondary antibodies (Santa Cruz Biotechnology, Heidelberg, Germany). Revelation was performed with ECL detection (Pierce, IllKirch, France), with a Bio-Rad imaging (Bio-Rad, Marnes la Coquette, France).

RT-qPCR. Total RNA was isolated from cell lines with RNeasy Plus mini kit (Qiagen, Courtaboeuf, France). Then 500 ng of total RNA was reverse transcribed by using the superscript III reverse transcriptase and random hexamers (Life Technologies). Quantitative PCR was done by using the Maxima SYBR Green/ROX qPCR Master Mix (Life Technologies) and the MX4000 instrument (Stratagene, Basel, Switzerland), according to the manufacturer's instructions. *RPLPO* 5′-AACCCAGCTCTGGAGAAACT-3′ (forward) and 5′-CCCCTGGAG ATTTTAGTGGT-3′ (reverse), *HPRT1* 5′-ATGCTGAGGATTTGGAAAGG-3′ (forward) and 5′-GATGTAATCCAGCAGGTCAGC-3′ (reverse), ACTB1 5′-AGAA AATCTGGCACCACACC-3′ (forward) and 5′-CAGAGGCGTACAGGGATAGC-3′ (reverse) and CDC20 5′-GGCGCTCCCATGGCACAGTT-3′ (forward) and 5′-CGGTCACCGCCAGGTTTGCT-3′ (reverse) were used for normalization. Relative quantification was carried out by using the ΔΔCt method.

BRET assay. Briefly, MCF-7 cells were seeded on 12-well plates and transfected with 50 ng/well of plasmid pRLuc-Bax coding for BRET donor and increasing amounts (for saturation curves) or 200 ng (for ABT-737 dose–response curves) of pS62A-eYFP-Bcl-xL or pS62D-eYFP-Bcl-xL mutants coding for BRET acceptor (or with corresponding pCMV-Bcl-xL for control). Twenty-four hours after transfection, cells were trypsinized and re-seeded into white a 96-well plate, incubated for another day, and then treated with drugs for 16 h (ABT-737 1 μM or increasing concentrations for dose–response curves). Light emission at 485 and 530 nm was measured consecutively by using the Mithras fluorescence-luminescence detector LB 940 (Berthold, Thoiry, France) after adding the luciferase substrate coelenterazine H (Uptima, MontLucon, France) at a final concentration of 5 μM, as described by Vo *et al.*[34] The BRET signal (mB.U, milliBRET Unit) was determined by calculating the ratio of the light emitted by the acceptor fusion protein eYFP-Bcl-xL (530 nm) over the light emitted by the donor fusion protein Rluc-Bax (475 nm). The values are corrected by subtracting the background signal detected when the donor constructs is expressed with the non-tagged acceptor Bcl-xL. For dose–response effect of ABT-737, %BRET is calculated using the following formula: $(BRET_{meas}-BRET_{min}) \times 100/(BRET_{max}-BRET_{min})$, where $BRET_{meas}$ is the BRET ratio obtained for every ABT737 concentration, $BRET_{min}$ is the BRET ratio measured at the highest ABT

concentration and $BRET_{max}$ is measured for untreated condition. All data were analysed using the commercial programme GraphPad PRISM 6.0 (GraphPad Software, La Jolla, CA, USA).

Immunofluorescence imaging. MCF-7 cells were plated onto glass coverslips and grown for 24 h before transfection with peYFP-Bcl-xL, pS62A-eYFP-Bcl-xL or pS62D-eYFP-Bcl-xL plasmids. Forty-eight hours after transfection, cells were stained with the cell-permeant MitoTracker probe (MitoTracker Red CMXRos, Invitrogen) as described by the manufacturer. Slides were then counterstained with DAPI and images were viewed on a Zeiss Axiovert 200 M microscope (MicroPIcell imaging facility).

Yeast assay. Yeast-expressing Bax and S62A or S62D-Bcl-xL were obtained by transforming the wild-type haploid strain BY4742 (*mata his3 leu2 lys2 ura3*) using pRS415-GPD-Bax plasmid under the control of the inducible *GAL1/10* promoter (*LEU2* as yeast selection marker) and p413-GPD-S62A-Bcl-xL or p413-GPD-S62D-Bcl-xL, coding for S62A-Bcl-xL or S62D-Bcl-xL, respectively, under the control of the constitutive GPD promoter (*HIS3* as yeast selection markers). Alternatively, Bax was expressed from the constitutive GPD promoter into the p415-GPD plasmid (*LEU2* as yeast selection marker). Cells were grown aerobically at 30 °C in a synthetic medium containing 0.67% yeast nitrogen base with ammonium sulfate (Difco), 0.01% of auxotrophic requirements, and 2% glucose as a carbon source on Petri dishes for 48 h or alternatively 2% raffinose and 2% galactose in 96-well plates with a starting cell density of 0.01 OD_{595} U/ml, in the presence of ABT-737 at 20 μM, or not. Cell density was measured at 24 h by OD_{595} and ratios between ABT-737-treated and untreated conditions were calculated for each Bcl-xL mutant. Yeast lysates were obtained as previously described.[28]

Statistics. Statistical analysis was performed by using one-tailed Student's *t*-test on R. Errors bars represent standard errors of the mean (S.E.M.). The symbols correspond to a *P*-value inferior to *0.05, **0.01 and ***0.001 and NS to statistically 'not significant'.

Conflict of Interest

The authors declare no conflict of interest.

1. Musacchio A, Salmon ED. The spindle-assembly checkpoint in space and time. *Nat Rev Mol Cell Biol* 2007; **8**: 379–393.
2. Weaver BAA, Cleveland DW. Decoding the links between mitosis, cancer, and chemotherapy: the mitotic checkpoint, adaptation, and cell death. *Cancer Cell* 2005; **8**: 7–12.
3. Brito DA, Rieder CL. Mitotic checkpoint slippage in humans occurs via cyclin B destruction in the presence of an active checkpoint. *Curr Biol* 2006; **16**: 1194–1200.
4. Gascoigne KE, Taylor SS. Cancer cells display profound intra- and interline variation following prolonged exposure to antimitotic drugs. *Cancer Cell* 2008; **14**: 111–122.
5. Huang HC, Shi J, Orth JD, Mitchison TJ. Evidence that mitotic exit is a better cancer therapeutic target than spindle assembly. *Cancer Cell* 2009; **16**: 347–358.
6. Symmans WF, Volm MD, Shapiro RL, Perkins AB, Kim AY, Demaria S *et al.* Paclitaxel-induced apoptosis and mitotic arrest assessed by serial fine-needle aspiration: implications for early prediction of breast cancer response to neoadjuvant treatment. *Clin Cancer Res* 2000; **6**: 4610–4617.
7. Juin P, Geneste O, Gautier F, Depil S, Campone M. Decoding and unlocking the Bcl-2 depencency of cancer cells. *Nat Rev Cancer* 2013; **13**: 455–465.
8. Oakes SR, Vaillant F, Lim E, Lee L, Breslin K, Feleppa F *et al.* Sensitization of Bcl-2 expressing breast tumors to chemotherapy by the BH3 mimetic ABT-737. *Proc Natl Acad Sci USA* 2012; **109**: 2766–2771.
9. Wei G, Margolin AA, Haery L, Brown E, Cucolo L, Julian B *et al.* Chemical genomics identifies small-molecule MCL1 repressors and BCL-xL as a predictor of MCL1 dependency. *Cancer Cell* 2012; **21**: 547–562.

10. Vaillant F, Merino D, Lee L, Breslin K, Pal B, Ritchie ME *et al*. Targeting Bcl-2 with the BH3 mimetic ABT-199 in estrogen receptor-positive breast cancer. *Cancer Cell* 2013; **24**: 120–129.

11. Oltersdorf T, Elmore SW, Shoemaker AR, Armstrong RC, Augeri DJ, Belli BA *et al*. An inhibitor of Bcl-2 family proteins induces regression of solid tumours. *Nature* 2005; **435**: 677–681.

12. Tse C, Shoemaker AR, Adickes J, Anderson MG, Chen J, Jin S *et al*. ABT-263: a potent and orally bioavailable Bcl-2 family inhibitor. *Cancer Res* 2008; **68**: 3421–3428.

13. Vo TT, Ryan J, Carrasco R, Neuberg D, Rossi DJ, Stone RM *et al*. Relative mitochondriel priming of myeloblasts and normal HSCs determines chemotherapeutic success in AML. *Cell* 2012; **151**: 344–355.

14. Ni Chonghaile T, Sarosiek KA, Vo TT, Ryan JA, Tammareddi A, Moore Vdel G *et al*. Pretreatment mitochondrial priming correlates with clinical response to cytotoxic chemotherapy. *Science* 2011; **334**: 1129–1133.

15. Kutuk O, Letai A. Alteration of the mitochondrial apoptotic pathway is key to acquired paclitaxel resistance and can be reversed by ABT-737. *Cancer Res* 2008; **68**: 7985–7994.

16. Barillé-Nion S, Bah N, Véquaud E, Juin P. Regulation of cancer cell survival by BCL2 family members upon prolonged mitotic arrest: opportunities for anticancer therapy. *Anticancer Res* 2012; **32**: 4225–4233.

17. Niikura Y, Dixit A, Scott R, Perkins G, Kitagawa K. BUB1 mediation of caspase-independent mitotic death determines cell fate. *J Cell Biol* 2007; **178**: 283–296.

18. Shi J, Zhou Y, Huang H-C, Mitchison TJ. Navitoclax (ABT-263) accelerates apoptosis during drug-induced mitotic arrest by antagonizing BCLXL. *Cancer Res* 2011; **71**: 4518–4526.

19. Tan N, Malek M, Zha J, Yue P, Kassees R, Berry L *et al*. Navitoclax enhances the efficacy of taxanes in non–small cell lung cancer models. *Clin Cancer Res* 2011; **17**: 1394–1404.

20. Wertz IE, Kusam S, Lam C, Okamoto T, Sandoval W, Anderson DJ *et al*. Sensitivity to antitubulin chemotherapeutics is regulated by MCL1 and FBW7. *Nature* 2011; **471**: 110–114.

21. Terrano DT, Upreti M, Chambers TC. Cyclin-dependent kinase 1-mediated BCLXL/BCL2 phosphorylation acts as a functional link coupling mitotic arrest and apoptosis. *Mol Cell Biol* 2010; **30**: 640–656.

22. Upreti M, Galitovskaya EN, Chu R, Tackett AJ, Terrano DT, Granell S *et al*. Identification of the major phosphorylation site in BCLXL induced by microtubule inhibitors and analysis of its functional significance. *J Biol Chem* 2008; **283**: 35517–35525.

23. Sakurikar N, Eichhorn JM, Chambers TC. Cyclin-dependent kinase-1 (Cdk1)/cyclin B1 dictates cell fate after mitotic arrest via phosphoregulation of antiapoptotic Bcl-2 proteins. *J Biol Chem* 2012; **287**: 39193–39204.

24. Basu A, Haldar S. Identification of a novel BCLXL phosphorylation site regulating the sensitivity of taxol- or 2-methoxyestradiol-induced apoptosis. *FEBS Lett* 2003; **538**: 41–47.

25. Wang J, Beauchemin M, Bertrand R. Phospho-Bcl-x(L)(Ser62) plays a key role at DNA damage-induced G(2) checkpoint. *Cell Cycle* 2012; **11**: 2159–2169.

26. Sakurikar N, Eichhorn JM, Alford SE, Chambers TC. Identification of a mitotic death signature in cancer cell lines. *Cancer Lett* 2014; **343**: 232–238.

27. Muchmore SW, Sattler M, Liang H, Meadows RP, Harlan JE, Yoon HS *et al*. X-ray and NMR structure of human Bcl-xL, an inhibitor of programmed cell death. *Nature* 1996; **381**: 335–341.

28. Gautier F, Guillemin Y, Cartron PF, Gallenne T, Cauquil N, Le Diguarher T *et al*. Bax activation by engagement with, then release from, the BH3 binding site of Bcl-xL. *Mol Cell Biol* 2011; **31**: 832–844.

29. Edlich F, Banerjee S, Suzuki M, Cleland MM, Arnoult D, Wang C *et al*. Bcl-x(L) retrotranslocates Bax from the mitochondria into the cytosol. *Cell* 2011; **145**: 104–116.

30. Kutuk O, Letai A. Displacement of Bim by Bmf and Puma rather than increase in Bim level mediates paclitaxel-induced apoptosis in breast cancer cells. *Cell Death Differ* 2010; **17**: 1624–1635.

31. Romagnoli M, Trichet V, David C, Clément M, Moreau P, Bataille R *et al*. Significant impact of survivin on myeloma cell growth. *Leukemia* 2007; **21**: 1070–1078.

32. Ryan J, Letai A. BH3 profiling in whole cells by fluorimeter or FACS. *Methods* 2013; **61**: 156–164.

33. Pan R, Hogdal LJ, Benito JM, Bucci D, Han L, Borthakur G *et al*. Selective BCL-2 inhibition by ABT-199 causes on-target cell death in acute myeloid leukemia. *Cancer Discov* 2014; **4**: 362–375.

34. Vo DD, Gautier F, Juin P, Grée R. Structure-activity relationship of selected polyphenol derivatives as inhibitors of Bax/Bcl-xL interaction. *Eur J Med Chem* 2012; **51**: 286–293.

Supplementary Information accompanies this paper on Cell Death and Disease website (http://www.nature.com/cddis)